To specify the CNP-interacting domain of Nogo-A, the protein extract of HEK293 cells, in which the transgenes encoding NIG and CNP were coexpressed, was processed for coimmunoprecipition analysis. To achieve this, the NIG gene or the full-length CNP gene was amplified by PCR, and cloned into the expression vector p3XFLAG-CMV7.1 (Sigma) or pCMV-Myc (Clontech, Mountain View, CA, USA) to express a fusion protein with an N-terminal Flag or Myc tag, respectively. After cotransfection of the vectors in HEK293 cells, the protein extract was processed for immunoprecipitation with mouse monoclonal anti-Flag M2 affinity gel (Sigma) or rabbit polyclonal anti-Myc-conjugated agarose (Sigma). This was followed by Western blot with rabbit polyclonal anti-Myc antibody (Sigma) and mouse monoclonal anti-FLAG M2 antibody (Sigma).

Cell imaging, immunocytochemistry and immunohistochemistry

To determine coexpression of NIG and CNP in neural cell cultures, the NIG gene or the full-length CNP was cloned into the expression vector pDsRed-Express-C1 (Clontech) or pFN2A CMV Flexi (Promega, Madison, WI, USA) to express a fusion protein with an N-terminal DsRed or Halo tag, respectively. They were cotransfected in SK-N-SH neuroblastoma cells. At 24–48 h after transfection, the cells were exposed to Oregon Green (Promega), a fluorochrome specifically bound to the Halo tag protein. In some experiments, primary cultures established from the brain of newborn Institute of Cancer Research (ICR) mice were processed for double-immunolabeling with anti-NIG antibody (AF3515) and anti-CNP antibody (11-5B), followed by labeling with Alexa Fluor 568-conjugated anti-sheep IgG (Invitrogen) and Alexa Fluor 488-conjugated anti-mouse IgG (Invitrogen). Subsequently, the cells were fixed briefly in 4% paraformaldehyde, exposed to 4′, 6′-diamidino-2-phenylindole (DAPI; Invitrogen), mounted on slides with glycerol-polyvinyl alcohol, and examined on the Olympus BX51 universal microscope.

For double-labeling immunohistochemistry, deparaffinated tissue sections were heated in 10 mmol/L citrate sodium buffer, pH 6.0 by autoclave for 30 s at 125°C in a temperature-controlled pressure chamber (Dako, Tokyo, Japan). They were incubated with PBS containing 10% normal goat serum for 15 min at room temperature (RT) to block non-specific staining. Then, tissue sections were stained at RT overnight with anti-CNP antibody (11-5B), followed by incubation with alkaline phosphatase (AP)-conjugated anti-mouse IgG (Nichirei, Tokyo, Japan), and colorized with New Fuchsin substrate. After inactivation of the antibody by autoclaving the sections at 125°C for 30 s in 10 mM citrate sodium buffer, pH 6.0, the tissue sections were treated for 15 min with 3% hydrogen peroxide-containing distilled water to block the endogenous peroxidase activity. Then, they were relabeled with anti-Nogo-A antibody (H-300) or anti-NIG antibody (AF-3515), followed by incubation with horseradish peroxidase (HRP)-conjugated secondary antibodies, and colorized with DAB substrate and a counterstain with hematoxylin. For negative controls, the step of incubation with primary antibodies was omitted.

RESULTS

Protein microarray-identified 82 NIG interactors

For protein microarray analysis, we prepared a highly purified V5-tagged NIG probe showing a single 45-kDa band in a 12% SDS-PAGE gel (Fig. 1a, lanes 1–3). By screening the protein microarray with this probe, we identified 82 proteins as those showing significant interaction with NIG among 5000 proteins on the array. They are listed in Table S2 online. Because Nogo-A is located not only on the plasma membrane of oligodendrocytes, but also in the ER where the NIG domain is exposed to the cytosol,[13] it is not surprising that many extramembrane proteins are listed in NIG-interacting partners.

Selection of CNP as the most probable NIG interactor candidate

First, for 82 NIG interactors, we investigated the EST profile on UniGene (http://www.ncbi.nlm.nih.gov/UniGene), the protein expression profile on Human Protein Reference Database (HPRD; http://www.hprd.org), and the mRNA expression profile of mouse orthologs in the brain on the Allen Brain Atlas (ABA) database (http://www.brain-map.org), a high-throughput *in situ* hybridization atlas of gene expression pattern in the adult mouse brain.[14] The database search suggested that the great majority of 82 NIG interactors represent non-neural proteins, suggesting the promiscuous binding of most NIG interactors in a non-physiological setting on the array. Therefore, we focused exclusively on the proteins whose expression in the CNS is supported by the expression profiling on UniGene, HRPD and ABA databases. Subsequently, we identified the proteins highly relevant to the biological function of Nogo-A by searching on PubMed by importing brain, neuron, neurite, axon, myelin, or oligodendrocyte as search terms. Following intensive search, we retrieved 12 neuron/oligodendrocyte-associated NIG interactors that were hit by any of these key words (Table 1). Among them, we finally found that only CNP (the spots in Fig. 1b), a cell type-specific marker for oligodendrocytes, has a physiological relevance to axon, myelin and oligodendrocytes (see the details in the Discussion section).

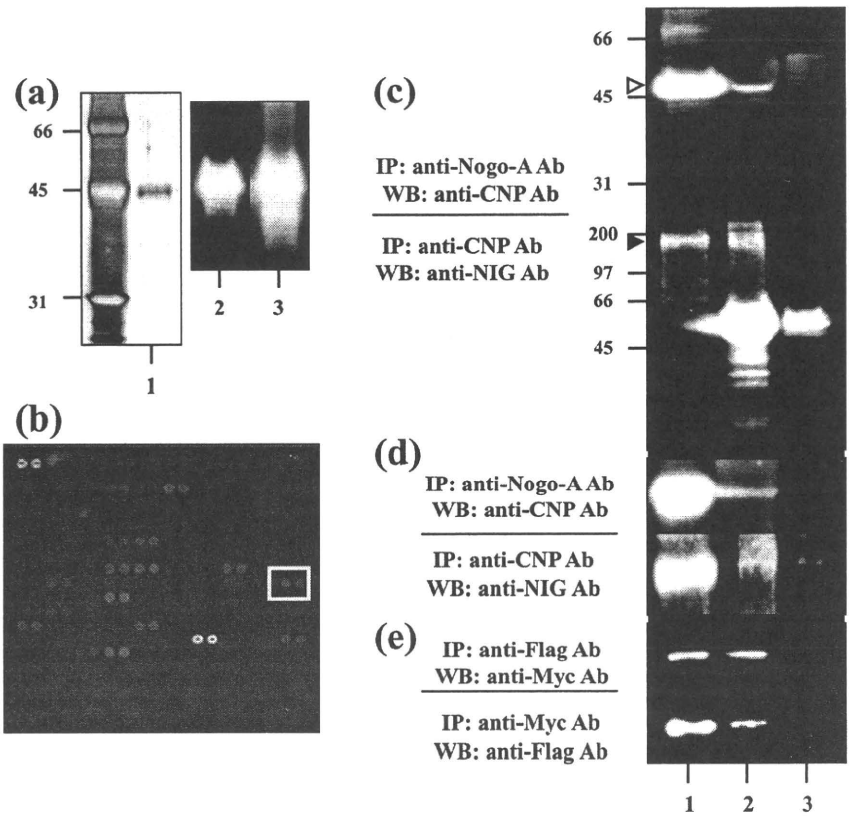

Fig. 1 Protein microarray and immunoprecipitation analysis. (a) The V5-tagged NIG-specific probe utilized for microarray analysis. The probe (0.3 μg each lane) was separated by a 12% SDS-PAGE gel. The silver stain of the gel with the position of molecular weight markers (lane 1). The blot was labeled with anti-V5 antibody (lane 2) and anti-human NIG antibody (lane 3). (b) Anti-2′, 3′-cyclic nucleotide 3′-phosphodiesterase (CNP) identified as a NIG interactor on the array. The protein microarray containing duplicate spots of 5000 proteins is composed of 4 × 12 subarrays. Each subarray includes 20 × 20 spots, composed of 76 control spots, including 14 positive and 62 negative control spots, 222 human target proteins, and 102 blanks and empty spots. The subarray No. 20 is shown. The spots positioned at row 10, columns 19, 20 indicated by an enclosed yellow line represent CNP. (c–e) Immunoprecipitation (IP) and Western blot (WB). Anti-Nogo-A antibody pulled down the endogenous CNP (open arrow, 47-kDa), while anti-CNP antibody precipitated the endogenous full-length Nogo-A (filled arrow, 190-kDa) from (c) the human brain homogenate, and from (d) the rat C6 glioma cell lysate. (e) The NIG gene and the CNP gene were cloned into the expression vectors to express a fusion protein with a Flag or Myc tag, respectively. They were cotransfected in HEK293 cells, and the lysate was processed for immunoprecipitation analysis with anti-Flag antibody and anti-Myc antibody. The lanes (1–3) of (c–e) represent (1) input control, (2) IP with the target-specific antibody, and (c) IP with normal mouse or rabbit IgG.

Validation of the interaction between NIG and CNP

Next, we verified the molecular interaction between Nogo-A and CNP by coimmunoprecipitation analysis. Anti-Nogo-A antibody (H-300) pulled down the endogenous CNP (47-kDa) labeled with anti-CNP antibody, while anti-CNP antibody (M-300) precipitated the full-length Nogo-A (190-kDa) labeled with anti-NIG antibody from both the human brain homogenate and the lysate of rat C6 glioma cells (Fig. 1c,d, upper and lower panels, lane 2). In contrast, the inclusion of normal IgG instead of H-300 or M-300 antibody recovered neither CNP nor Nogo-A (Fig. 1c,d, upper and lower panels, lane 3), supporting the specificity of the interaction. These results indicate that the endogenous Nogo-A interacts with the endogenous CNP *in vitro* and *in vivo*.

To specify the CNP-interacting domain of Nogo-A, the NIG gene or the CNP gene was cloned into the two different expression vectors to express a fusion protein with an N-terminal Flag or Myc tag. After cotransfection of the vectors in HEK293 cells, the protein extract was processed for immunoprecipitation with mouse monoclonal anti-Flag M2 affinity gel, rabbit polyclonal anti-Myc-conjugated agarose, or the same amount of normal mouse or rabbit IgG-conjugated agarose, followed by Western blot with rabbit polyclonal anti-Myc antibody and mouse monoclonal anti-FLAG M2 antibody. The reciprocal coimmunoprecipitation analysis verified the interaction of the NIG domain of Nogo-A and CNP (Fig. 1e, upper and lower panels, lane 2). These results indicate that the NIG domain of Nogo-A on its own interacts with CNP, but do not exclude the possibility that the domain located outside NIG is also bound to CNP.

To determine subcellular colocation of NIG and CNP, the NIG gene or the CNP gene was cloned into the two different expression vectors to express a fusion protein with an N-terminal DsRed or Halo tag. When cotransfected in SK-N-SH neuroblastoma cells, NIG was expressed not only on the plasma membrane but also in the cytoplasm, and at low amounts in the nucleus. DsRed-tagged NIG and Oregon Green-labeled CNP were coexpressed chiefly in the cytoplasm (Fig. 2, panels a–c). Furthermore, coexpression of NIG and CNP was identified

Table 1 Twelve neuron/oligodendrocyte-associated NIG interactors

No.	Gene symbol	Gene name	Z-score	Putative function
1	RPL31	Ribosomal protein L31	7.22386	A ribosomal protein that constitutes a component of the 60S subunit
2	CIRBP	Cold inducible RNA binding protein	6.76639	A cold-shock protein that plays a role in cold-induced suppression of cell proliferation
3	PLK3	Polo-like kinase 3 (Drosophila)	6.51572	A serine/threonine kinase that plays a role in regulation of cell cycle progression
4	MARK4	MAP/microtubule affinity-regulating kinase 4	5.45038	A serine/threonine kinase involved in microtubule organization in neuronal cells
5	RPL30	Ribosomal protein L30	4.82371	A ribosomal protein that constitutes a component of the 60S subunit
6	CNP	2',3'-cyclic nucleotide 3' phosphodiesterase	4.71717	A membrane-bound enzyme located in the CNS myelin
7	FGF13	Fibroblast growth factor 13	4.35684	A member of the fibroblast growth factor family
8	ZNF192	Zinc finger protein 192	4.09363	A transcription factor of unknown function
9	NHP2	Nucleolar protein family A, member 2 (H/ACA small nucleolar RNPs)	4.04663	A member of the H/ACA snoRNPs gene family
10	ATP5O	ATP synthase, H+ transporting, mitochondrial F1 complex, O subunit (oligomycin sensitivity conferring protein)	3.25389	A component of the F-type ATPase located in the mitochondrial matrix
11	ODC1	Ornithine decarboxylase 1	3.06902	The rate-limiting enzyme of the polyamine biosynthesis pathway that catalyzes ornithine to putrescine
12	EIF2C1	Eukaryotic translation initiation factor 2C, 1	3.00322	A member of the Argonaute family that plays a role in RNA interference

Among 82 NIG interactor candidates (Table S2), 12 were categorized as neuron/oligodendrocyte-associated NIG interactors by database search on UniGene, HPRD, and Allen Brain Atlas, and by the PubMed search with brain, neuron, neurite, axon, myelin, or oligodendrocyte as search terms. Among them, we found that only CNP (No. 6) has a physiological relevance to axon, myelin and oligodendrocytes.

both in the cytoplasm and on the cell surface of highly-branched differentiated oligodendrocytes consisting of a small population of newborn mouse brain cell cultures (Fig. 2, panels d–f).

Finally, we studied coexpression of Nogo-A and CNP *in vivo* in the human brain by immunohistochemistry. A substantial overlap was found in the expression pattern of Nogo-A, NIG and CNP in oligodendrocytes and myelin sheaths of the cerebral white matter (Fig. 2, panels g and h), supporting the possibility that Nogo-A *in vivo* interacts with CNP, probably by binding via the NIG domain.

DISCUSSION

Protein microarray serves as a powerful tool for the rapid and systematic identification of protein-protein and other biomolecule interactions.[10] Protein microarray has a wide range of applications, including characterization of antibody specificity and autoantibody repertoire, and identification of novel biomarkers and molecular targets associated with disease type, stage and progression, leading to establishment of personalized medicine.[10] When a specific probe is available, the whole experimental procedure of protein microarray analysis requires the exact time shorter than 5 h to obtain the complete list of interacting proteins on the array.[11,12]

However, protein microarray technology is still under development in methodological aspects.[10–12] In general, protein microarray has its own limitations associated with the expression and purification of a wide variety of target proteins. In the microarray we utilized, the target proteins were expressed in a baculovirus expression system, purified under native conditions, and spotted on the slides to ensure the preservation of native structure, post-translational modifications such as glycosylation and phophorylation, and proper functionality. In contrast, bacterially expressed proteins lack glycosylation and phosphorylation moieties, and are often misfolded during purification. Since target proteins contain a GST fusion tag, the arrays are always processed for the post-spotting quality control by using an anti-GST antibody with a concentration gradient of GST spots as a standard. This procedure makes it possible to quantify the exact amount of proteins deposited in each spot, and thereby minimizes the inter-lot variability of the results. Furthermore, each subarray contains a series of built-in control spots.

Protein microarray also has another technical limitation attributable to the avidity of protein-protein interaction.[10–12] The probing and rigorous washing procedure detects mostly the direct protein-protein interaction supported by the stable binding ability. It could not efficiently detect much weak and transient protein-protein interactions, or indirect interactions that require accessory molecules or intervening cofactors. In addition,

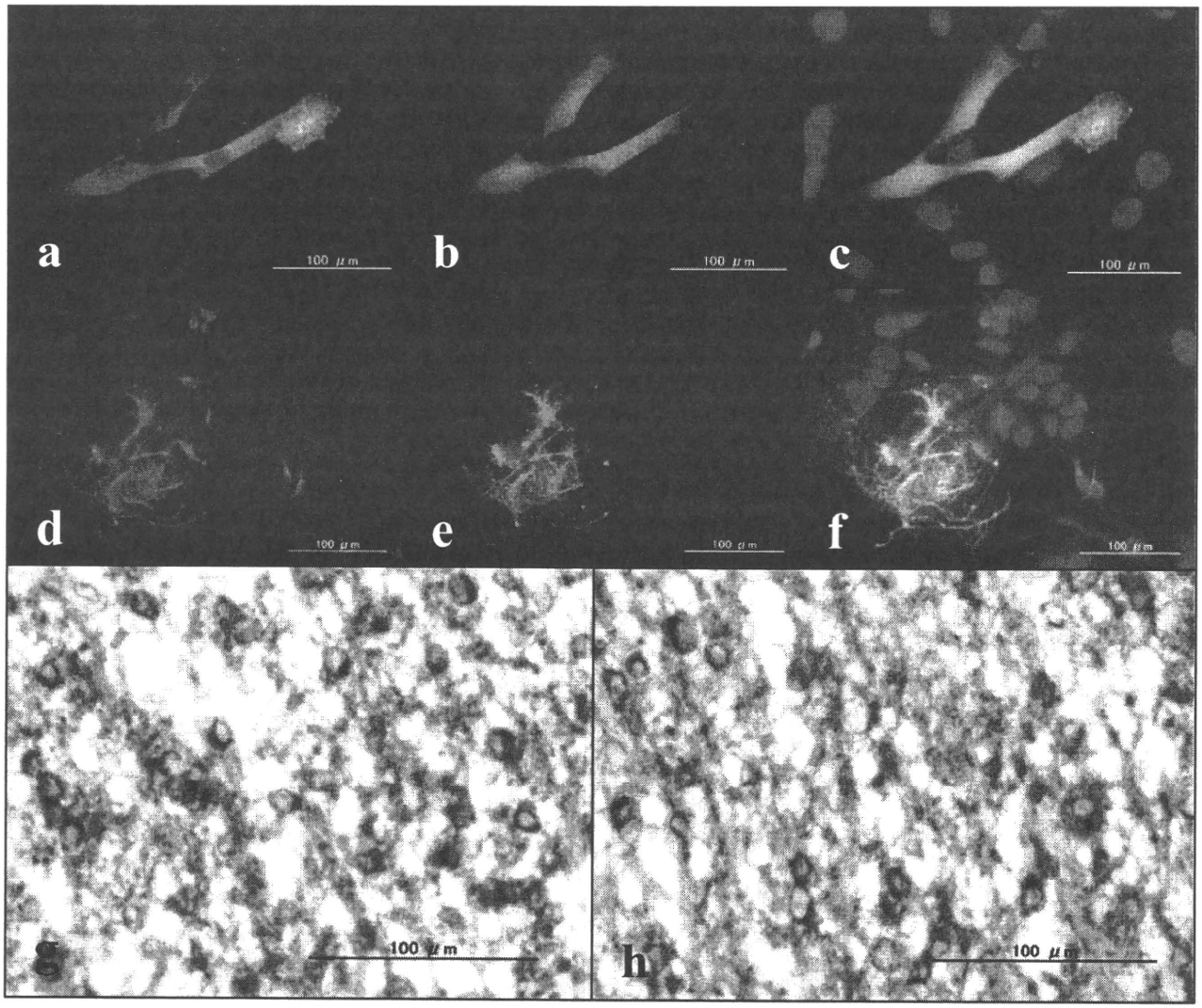

Fig. 2 Coexpression of NIG and anti-2′, 3′-cyclic nucleotide 3′-phosphodiesterase (CNP). (a–c) SK-N-SH neuroblastoma cells. The NIG gene and the CNP gene were cloned into the expression vectors to express a fusion protein with a DsRed or Halo tag, and they were cotransfected in SK-N-SH cells. (a) DsRed-labeled NIG, (b) Oregon Green-labeled CNP, and (c) merge (a) and (b) with 4′, 6′-diamidino-2-phenylindole (DAPI). (d–f) Newborn mouse brain cell cultures. Primary cultures established from newborn ICR mice double immunolabeled with anti-NIG antibody (AF3515) and anti-CNP antibody (11-5B), followed by labeling with Alexa Fluor 568-conjugated anti-sheep IgG and Alexa Fluor 488-conjugated anti-mouse IgG. (d) NIG, (e) CNP, and (f) merge (d) and (e) with DAPI. (g,h) Human brain tissues. The human brain tissue section derived from the peri-infarct white matter of the frontal cortex of a 62-year-old male with middle cerebral artery occlusion was double immunolabeled with (g) anti-Nogo-A antibody (H-300; brown) and anti-CNP antibody (11-5B; red) and (h) anti-NIG antibody (AF3515; brown) and anti-CNP antibody (11-5B; red).

protein microarray screening does not consider the specific subcellular location where the protein-protein interaction actually takes place. Thus, it is possible that some promiscuous partners are detected, whereas some biologically important interactors *in vivo* are left beyond identification. Therefore, protein microarray data always require the validation by other independent methods such as coimmunoprecipitation, Western blotting, the yeast two-hybrid (Y2H) screening, and so on. Post-translational modifications play a pivotal role in a range of protein-protein interactions. Immunolabeling of the array we utilized with anti-phosphotyrosine antibody showed that approximately 10–20% of the proteins on the array are phosphorylated (unpublished data of Invitrogen). When the array was applied for kinase substrate identification, most known kinases immobilized on the array are enzymatically active with the capacity of autophosphorylation, suggesting that they are functionally

active with preservation of proper conformation (unpublished data of Invitrogen).

Previous studies indicate that the central domain of Amino-Nogo spanning amino acids 567–748 in the human Nogo-A designated NIG mediates persistent inhibition of axonal outgrowth and induces growth cone collapse by signaling through an as yet unidentified NIG receptor.[3] To characterize NIG-interacting proteins that might include an NIG receptor, we screened the high-density human protein microarray composed of 5000 proteins with a recombinant NIG protein as a probe. However, most of the 82 NIG interactors identified by protein microarray analysis are non-neural proteins, suggesting promiscuous binding in a non-physiological setting on the array. Therefore, we focused exclusively on the proteins whose expression in the CNS is supported by the expression profiling on UniGene, HRPD and ABA databases. Subsequently, we searched them on PubMed and retrieved 12 neuron/oligodendrocyte-associated NIG interactors (Table 1). Among them, we finally identified CNP as the most probable candidate in view of a physiological relevance to axon, myelin and oligodendrocytes. CNP is a valid cell type-specific marker for oligodendrocytes, essential for axonal support but not for myelin assembly.[15] CNP acts as a membrane anchor for tubulin required for process outgrowth of oligodendrocytes,[16,17] and ubiquitinated CNP is concentrated within lipid rafts,[18] suggesting that CNP expressed intracellularly in the cytoplasm is located in close proximity to the cell membrane where Nogo-A is accumulated. Therefore, we considered CNP as the most feasible NIG interactor candidate *in vivo*. The interaction of NIG with CNP and their coexpression in both oligodendrocytes and myelin were validated by immunoprecipitation, cell imaging, and immunolabeling.

Previously, we and others showed that Nogo-A expression is greatly enhanced in surviving oligodendrocytes and CNP is expressed in damaged but still remaining myelin sheaths, while NgR is upregulated in reactive astrocytes and macrophages/microglia at the edge of chronic active demyelinating lesions of multiple sclerosis (MS),[19,20] suggesting a pathological role of Nogo-A/NgR interaction in persistent demyelination and loss of axonal regeneration in MS lesions. Interestingly, a certain population of MS patients shows enhanced T-cell and B-cell responses against CNP and Nogo-A, suggesting that both CNP and Nogo-A serve as autoantigens.[21,22] Nogo-A takes at least two different membrane topologies in oligodendrocytes,[3,8] where it is possible that the N-terminal region of Nogo-A is exposed to the extracellular space or is located in the cytoplasm. Because CNP is expressed primarily in the cytoplasm of oligodendrocytes, it might not serve as a cell-surface NIG receptor possibly expressed on axons and neurons that transduces the signals for inhibition of axonal outgrowth and induction of growth cone collapse. However, the possibility exists that CNP could act as an intracellular conformational stabilizer for the intrinsically-unstructured unstable Amino-Nogo segment in oligodendrocytes (Fig. 3).

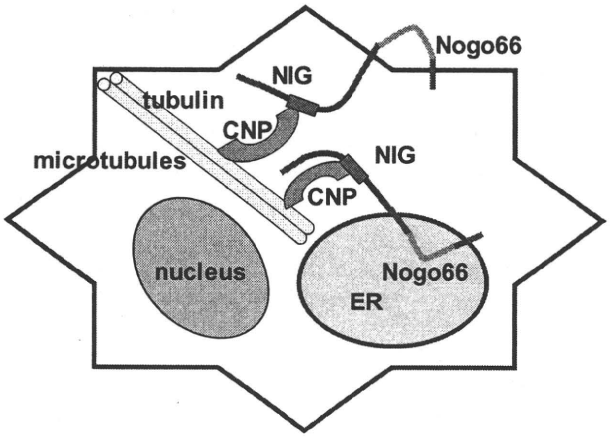

Fig. 3 A hypothetical model of NIG and anti-2′, 3′-cyclic nucleotide 3′-phosphodiesterase (CNP) interaction in oligodendrocytes. CNP (the orange piece) acts as a membrane anchor for tubulin essential for process outgrowth of oligodendrocytes, located in close proximity to the plasma membrane and possibly to the ER membrane where Nogo-A is accumulated. By interacting with NIG (the grey box), CNP serves as an intracellular conformational stabilizer for the intrinsically unstructured large segment of Amino-Nogo.

ACKNOWLEDGMENTS

All autopsied brain samples obtained under written informed consent were provided by Research Resource Network (RRN), Japan. This work was supported by a research grant to J-IS from the High-Tech Research Center Project, the Ministry of Education, Culture, Sports, Science and Technology (MEXT), Japan (S0801043).

REFERENCES

1. Walmsley AR, Mir AK. Targeting the Nogo-a signalling pathway to promote recovery following acute CNS injury. *Curr Pharm Des* 2007; **13**: 2470–2484.
2. Pernet V, Joly S, Christ F, Dimou L, Schwab ME. Nogo-A and myelin-associated glycoprotein differently regulate oligodendrocyte maturation and myelin formation. *J Neurosci* 2008; **28**: 7435–7444.
3. Oertle T, van der Haar ME, Bandtlow CE *et al.* Nogo-A inhibits neurite outgrowth and cell spreading with three discrete regions. *J Neurosci* 2003; **23**: 5393–5406.

4. Li M, Song J. The N- and C-termini of the human Nogo molecules are intrinsically unstructured: bioinformatics, CD, NMR characterization, and functional implications. *Proteins* 2007; **68**: 100–108.
5. Zander H, Hettich E, Greiff K, Chatwell L, Skerra A. Biochemical characterization of the recombinant human Nogo-A ectodomain. *FEBS J* 2007; **274**: 2603–2613.
6. Schweigreiter R, Walmsley AR, Niederöst B *et al.* Versican V2 and the central inhibitory domain of Nogo-A inhibit neurite growth via p75NTR/NgR-independent pathways that converge at RhoA. *Mol Cell Neurosci* 2004; **27**: 163–174.
7. Freund P, Schmidlin E, Wannier T *et al.* Nogo-A-specific antibody treatment enhances sprouting and functional recovery after cervical lesion in adult primates. *Nat Med* 2006; **12**: 790–792.
8. Dodd DA, Niederoest B, Bloechlinger S, Dupuis L, Loeffler JP, Schwab ME. Nogo-A, -B, and -C are found on the cell surface and interact together in many different cell types. *J Biol Chem* 2005; **280**: 12494–12502.
9. Hu F, Strittmatter SM. The N-terminal domain of Nogo-A inhibits cell adhesion and axonal outgrowth by an integrin-specific mechanism. *J Neurosci* 2008; **28**: 1262–1269.
10. Schweitzer B, Predki P, Snyder M. Microarrays to characterize protein interactions on a whole-proteome scale. *Proteomics* 2003; **3**: 2190–2199.
11. Satoh J, Nanri Y, Yamamura T. Rapid identification of 14-3-3-binding proteins by protein microarray analysis. *J Neurosci Methods* 2006; **152**: 278–288.
12. Satoh J, Obayashi S, Misawa T, Sumiyoshi K, Oosumi K, Tabunoki H. Protein microarray analysis identifies human cellular prion protein interactors. *Neuropathol Appl Neurobiol* 2009; **35**: 16–35.
13. Voeltz GK, Prinz WA, Shibata Y, Rist JM, Rapoport TA. A class of membrane proteins shaping the tubular endoplasmic reticulum. *Cell* 2006; **124**: 573–586.
14. Lein ES, Hawrylycz MJ, Ao N *et al.* Genome-wide atlas of gene expression in the adult mouse brain. *Nature* 2007; **445**: 168–176.
15. Lappe-Siefke C, Goebbels S, Gravel M *et al.* Disruption of Cnp1 uncouples oligodendroglial functions in axonal support and myelination. *Nat Genet* 2003; **33**: 366–374.
16. Bifulco M, Laezza C, Stingo S, Wolff J. 2′,3′-Cyclic nucleotide 3′-phosphodiesterase: a membrane-bound, microtubule-associated protein and membrane anchor for tubulin. *Proc Natl Acad Sci USA* 2002; **99**: 1807–1812.
17. Lee J, Gravel M, Zhang R, Thibault P, Braun PE. Process outgrowth in oligodendrocytes is mediated by CNP, a novel microtubule assembly myelin protein. *J Cell Biol* 2005; **170**: 661–673.
18. Hinman JD, Chen CD, Oh SY, Hollander W, Abraham CR. Age-dependent accumulation of ubiquitinated 2′, 3′-cyclic nucleotide 3′-phosphodiesterase in myelin lipid rafts. *Glia* 2008; **56**: 118–133.
19. Satoh J, Onoue H, Arima K, Yamamura T. Nogo-A and nogo receptor expression in demyelinating lesions of multiple sclerosis. *J Neuropathol Exp Neurol* 2005; **64**: 129–138.
20. Kuhlmann T, Remington L, Maruschak B, Owens T, Brück W. Nogo-A is a reliable oligodendroglial marker in adult human and mouse CNS and in demyelinated lesions. *J Neuropathol Exp Neurol* 2007; **66**: 238–246.
21. Muraro PA, Kalbus M, Afshar G, McFarland HF, Martin R. T cell response to 2′,3′-cyclic nucleotide 3′-phosphodiesterase (CNPase) in multiple sclerosis patients. *J Neuroimmunol* 2002; **130**: 233–242.
22. Onoue H, Satoh JI, Ogawa M, Tabunoki H, Yamamura T. Detection of anti-Nogo receptor autoantibody in the serum of multiple sclerosis and controls. *Acta Neurol Scand* 2007; **115**: 153–160.

SUPPORTING INFORMATION

Additional Supporting Information may be found in the online version of this article:

Table S1 The complete list of the proteins immobilized on a human protein microarray utilized in the present study
Table S2 The list of 82 NIG interactors identified by protein microarray

Please note: Wiley-Blackwell are not responsible for the content or functionality of any supporting materials supplied by the authors. Any queries (other than missing material) should be directed to the corresponding author for the article.

Clinical and Experimental Neuroimmunology 1 (2010) 127–140

REVIEW ARTICLE

Bioinformatics approach to identifying molecular biomarkers and networks in multiple sclerosis

Jun-ichi Satoh

Department of Bioinformatics and Molecular Neuropathology, Meiji Pharmaceutical University, Tokyo, Japan

Keywords
bioinformatics; KeyMolnet; molecular network; multiple sclerosis; systems biology

Correspondence
Jun-ichi Satoh MD, PhD, Department of Bioinformatics and Molecular Neuropathology, Meiji Pharmaceutical University,
2-522-1 Noshio, Kiyose, Tokyo 204-8588, Japan.
Tel: +81-42-495-8678
Fax: +81-42-495-8678
Email: satoj@my-pharm.ac.jp

Received: 6 June 2010; accepted: 3 August 2010.

Abstract

Multiple sclerosis (MS) is an inflammatory demyelinating disease of the central nervous system (CNS) white matter mediated by an autoimmune process triggered by a complex interplay between genetic and environmental factors, in which the precise molecular pathogenesis remains to be comprehensively characterized. The global analysis of genome, transcriptome, proteome and metabolome, collectively termed omics, promotes us to characterize the genome-wide molecular basis of MS. However, as omics studies produce high-throughput experimental data at one time, it is often difficult to find out the meaningful biological implications from huge datasets. Recent advances in bioinformatics and systems biology have made major breakthroughs by illustrating the cell-wide map of complex molecular interactions with the aid of the literature-based knowledgebase of molecular pathways. The integration of omics data derived from the disease-affected cells and tissues with underlying molecular networks provides a rational approach not only to identifying the disease-relevant molecular markers and pathways, but also to designing the network-based effective drugs for MS. (Clin. Exp. Neuroimmunol. doi: 10.1111/j.1759-1961.2010.00013.x, September 2010)

Introduction

Multiple sclerosis (MS) is an inflammatory demyelinating disease affecting exclusively the central nervous system (CNS) white matter mediated by an autoimmune process triggered by a complex interplay between genetic and environmental factors.[1] Intravenous administration of interferon-gamma (IFNγ) provoked acute relapses of MS, indicating a pivotal role of proinflammatory T helper type 1 (Th1) lymphocytes. More recent studies proposed the pathogenic role of Th17 lymphocytes in sustained tissue damage in MS.[2] MS shows a great range of phenotypic variability. The disease is classified into relapsing-remitting MS (RRMS), secondary progressive MS (SPMS) or primary progressive MS (PPMS) with respect to the clinical course. Pathologically, MS shows a remarkable heterogeneity in the degree of inflammation, complement activation, antibody deposition, demyelination and remyelination, oligodendrocyte apoptosis, and axonal degeneration.[3] Currently available drugs in clinical practice of MS, including interferon-beta (IFNβ), glatiramer acetate, mitoxantrone, FTY720 and natalizumab, have proven only limited efficacies in subpopulations of the patients.[4] These observations suggest the hypothesis that MS is a kind of neurological syndrome caused by different immunopathological mechanisms leading to the final common pathway that provokes inflammatory demyelination. Therefore, the identification of specific biomarkers relevant to the heterogeneity of MS is highly important to establish the molecular mechanism-based personalized therapy in MS.

After the completion of the Human Genome Project in 2003, the global analysis of genome, transcriptome, proteome and metabolome, collectively termed omics, promotes us to characterize the genome-wide molecular basis of the diseases, and helps us to identify disease-specific molecular signatures

and biomarkers for diagnosis and prediction of prognosis. Actually, the genome-wide association study (GWAS) of MS revealed novel risk alleles for susceptibility of MS.[5] The comprehensive transcriptome and proteome profiling of brain tissues and lymphocytes identified key molecules aberrantly regulated in MS, whose role has not been previously predicted in the pathogenesis of MS.[6,7] Most recently, the application of next-generation sequencing technology to personal genomes has enabled us to investigate the genetic basis of MS at the level of individual patients.[8]

Because omics studies usually produce high-throughput experimental data at one time, it is often difficult to find out the meaningful biological implications from such a huge dataset. Recent advances in bioinformatics and systems biology have made major breakthroughs by showing the cell-wide map of complex molecular interactions with the aid of the literature-based knowledgebase of molecular pathways.[9] The logically arranged molecular networks construct the whole system characterized by robustness, which maintains the proper function of the system in the face of genetic and environmental perturbations.[10] In the scale-free molecular network, targeted disruption of limited numbers of critical components designated the hub, on which the biologically important molecular connections concentrate, could disturb the whole cellular function by destabilizing the network.[11] From the point of these views, the integration of omics data derived from the disease-affected cells and tissues with underlying molecular networks provides a rational approach not only to characterizing the disease-relevant pathways, but also to identifying the network-based effective drug targets.

Increasing numbers of human disease-oriented omics data have been deposited in public databases, such as the Gene Expression Omnibus (GEO) repository (http://www.ncbi.nlm.nih.gov/geo) and the ArrayExpress archive (http://www.ebi.ac.uk/microarray-as/ae). Most of these are transcriptome datasets. Importantly, they really include the data that have potentially valuable information on molecular biomarkers and networks of the diseases, when they are reanalyzed by appropriate bioinformatics approaches, followed by validation of *in silico* observations with *in vitro* and *in vivo* experiments.[12]

The present review has focused on bioinformatics approaches to identifying MS-associated molecular biomarkers and networks from high-throughput data of omics studies.

Global gene expression analysis

DNA microarray technology is an innovative approach that allows us to systematically monitor the genome-wide gene expression pattern of disease-affected tissues and cells. This approach enables us to illustrate most efficiently a global picture of cellular activity by the messenger RNA (mRNA) expression levels as an indicator, although the levels of mRNA do not always correlate with the levels of proteins directly involved in cellular function. However, the use of DNA microarray is more convenient to collect temporal and spatial snapshots of gene expression than the conventional mass spectrometry, which is often hampered by limited resolution of protein separation. In transcriptome analysis, we could logically assume that a set of coregulated genes might have similar biological functions within the cells.

First of all, I would like to briefly overview the gene expression analysis (Fig. 1). In general, total RNA fractions containing mRNA species are extracted from cells and tissues, individually labeled with fluorescent dyes, and processed for hybridization with thousands of oligonucleotides of known sequences immobilized on the arrays. After washing, they are processed for signal acquisition on a scanner. Various types of microarrays are currently available, although the MicroArray Quality Control (MAQC) project verified that the core results are well reproducible among different platforms used.[13] However, it is recommended that each experiment should contain biological replicates to validate reproducibility of the observations. The raw data are normalized by representative methods, including the quantile normalization method and the Robust MultiChip Average (RMA) method using the R software of the Bioconductor package (cran.r-project.org) or the GeneSpring software (Agilent Technology, Palo Alto, CA, USA).

To identify differentially expressed genes (DEG) among distinct samples, the normalized data are processed for statistical analysis using *t*-test for comparison between two groups or analysis of variance (ANOVA) for comparison among more than three groups, followed by the multiple comparison test with the Bonferroni correction or by controlling false discovery rate (FDR) below 0.05 to adjust *P*-values.

In the next step, the levels of expression of DEG should be validated by quantitative reverse transcription polymerase chain reaction (qRT–PCR). The normalized data are also processed for hierarchical

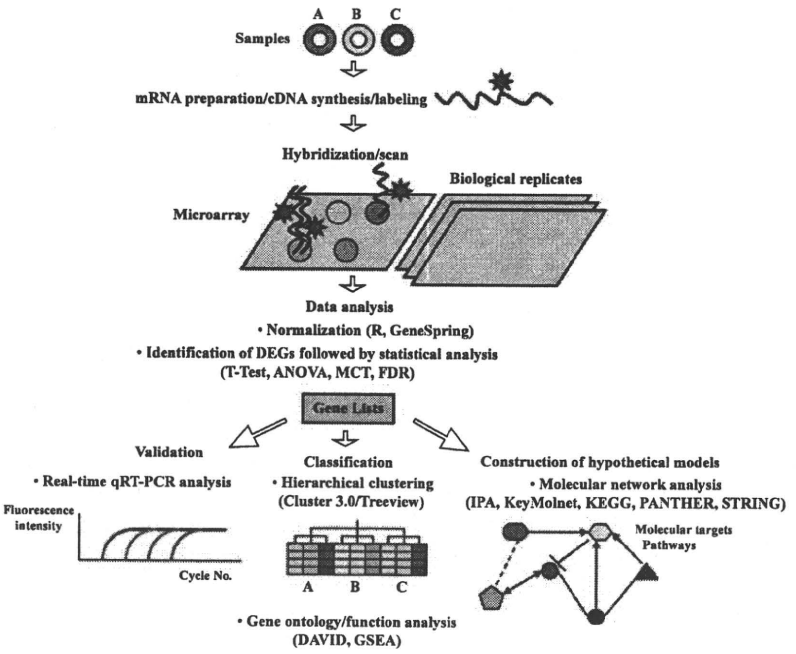

Figure 1 The load map from global gene expression profiling to molecular network analysis. Total RNA samples labeled with fluorescent dyes are processed for hybridization with oligonucleotide probes on the arrays, which should include biological replicates. They are processed for signal acquisition on a scanner. To identify the list of differentially expressed genes (DEG) among the samples, the normalized data are processed for statistical analysis, followed by validation by quantitative reverse transcription polymerase chain reaction (qRT–PCR). They are also processed for hierarchical clustering analysis and gene ontology and function analysis. To identify biologically relevant molecular pathways, the list of DEG is imported into pathway analysis tools endowed with a comprehensive knowledgebase. ANOVA, analysis of variance; DAVID, Database for Annotation, Visualization and Integrated Discovery; FDR, false discovery rate; GSEA, Gene Set Enrichment Analysis; IPA, Ingenuity Pathways Analysis; KEGG, Kyoto Encyclopedia of Genes and Genomes; MCT, multiple comparison test; PANTHER, Protein Analysis Through Evolutionary Relationships; and STRING; Search Tool for the Retrieval of Interacting Genes/Proteins.

clustering analysis to classify the expression of profile-based groups of genes and samples by using GeneSpring or the open-access resources, such as Cluster 3.0 (bonsai.ims.u-tokyo.ac.jp/~mdehoon/software/cluster) and TreeView (sourceforge.net/projects/jtreeview). The Gene ID Conversion tool of the Database for Annotation, Visualization and Integrated Discovery (DAVID) (david.abcc.ncifcrf.gov)[14] converts the large-scale array-specific probe IDs into the corresponding Entrez Gene IDs, HUGO Gene Symbols, Ensembel Gene IDs or UniProt IDs, being more convenient for application to the downstream analysis. Both the DAVID Functional annotation tool and the Gene Set Enrichment Analysis (GSEA) tool (www.broad.mit.edu/gsea/downloads.jsp)[15] are open-access resources that help us to identify a set of enriched genes with a specified functional annotation in the entire list of genes. Many other approaches for preprocessing microarray data are applicable, and the resources are available elsewhere.

Molecular network analysis

To identify biologically relevant molecular pathways from large-scale data, we could analyze them by using a battery of pathway analysis tools endowed with a comprehensive knowledgebase; that is, Kyoto Encyclopedia of Genes and Genomes (KEGG; http://www.kegg.jp), the Protein Analysis Through Evolutionary Relationships (PANTHER) classification system (http://www.pantherdb.org), Search Tool for the Retrieval of Interacting Genes/Proteins (STRING; string.embl.de), Ingenuity Pathways Analysis (IPA; Ingenuity Systems, http://www.ingenuity.com) and KeyMolnet (Institute of Medicinal Molecular Design, http://www.immd.co.jp) (Fig. 1). KEGG, PANTHER and STRING are open-access databases, whereas IPA and KeyMolnet are commercial databases updated regularly. Both transcriptome and proteome data are acceptable for all the databases described here.

KEGG systematically integrates genomic and chemical information to create the whole biological

system *in silico*.[16] KEGG includes manually curated reference pathways that cover a wide range of metabolic, genetic, environmental and cellular processes, and human diseases. Currently, KEGG contains 108 983 pathways generated from 358 reference pathways. PANTHER, operating on the computational algorithms that relate the evolution of protein sequences to the evolution of protein functions and biological roles, provides a structured representation of protein function in the context of biological reaction networks.[17] PANTHER includes the information on 165 regulatory and metabolic pathways, manually curated by expert biologists. By uploading the list of Gene IDs, the PANTHER gene expression data analysis tool identifies the genes in terms of over- or under-representation in canonical pathways, followed by statistical evaluation by multiple comparison test with the Bonferroni correction. STRING is a database that contains physiological and functional protein-protein interactions composed of 2 590 259 proteins from 630 organisms.[18] STRING integrates the information from numerous sources, including experimental repositories, computational prediction methods and public text collections. By uploading the list of UniProt IDs, STRING illustrates the union of all possible association networks.

IPA is a knowledgebase that contains approximately 2 270 000 biological and chemical interactions and functional annotations with definite scientific evidence, curated by expert biologists.[19] By uploading the list of Gene IDs and expression values, the network-generation algorithm identifies focused genes integrated in a global molecular network. IPA calculates the score *P*-value, the statistical significance of association between the genes and the networks by the Fisher's exact test.

KeyMolnet contains knowledge-based content on 123 000 relationships among human genes and proteins, small molecules, diseases, pathways and drugs, curated by expert biologists.[20] They are categorized into the core content collected from selected review articles with the highest reliability or the secondary contents extracted from abstracts of PubMed and Human Reference Protein database (HPRD). By importing the list of Gene ID and expression values, KeyMolnet automatically provides corresponding molecules as a node on networks. The "common upstream" network-search algorithm enables us to extract the most relevant molecular network composed of the genes coordinately regulated by putative common upstream transcription factors. The "neighboring" network-search algorithm selected one or more molecules as starting points to generate the network of all kinds of molecular interactions around starting molecules, including direct activation/inactivation, transcriptional activation/repression, and the complex formation within the designated number of paths from starting points. The "N-points to N-points" network-search algorithm identifies the molecular network constructed by the shortest route connecting the start-point molecules and the end-point molecules. The generated network was compared side-by-side with 430 human canonical pathways of the KeyMolnet library. The algorithm counting the number of overlapping molecular relations between the extracted network and the canonical pathway makes it possible to identify the canonical pathway showing the most significant contribution to the extracted network. The significance in the similarity between both is scored following the formula, where O is the number of overlapping molecular relations between the extracted network and the canonical pathway, V is the number of molecular relations located in the extracted network, C is the number of molecular relations located in the canonical pathway, T is the number of total molecular relations, and X is the sigma variable that defines coincidence.

$$\text{Score} = -\log_2(\text{Score}[P])$$

$$\text{Score}(P) = \sum_{x=O}^{\text{Min}(C,V)} f(x)$$

$$f(x) = {}_C C_x \cdot {}_{T-C} C_{V-x} / {}_T C_V$$

Biomarkers for predicting MS relapse

Molecular mechanisms underlying acute relapse of MS remain currently unknown. If molecular biomarkers for MS relapse are identified, we could predict the timing of relapses, being invaluable to start the earliest preventive intervention.

By gene expression profiling with Affymetrix Human Genome U133 plus 2.0 arrays, Corvol et al. identified 975 genes that separate clinically isolated syndrome (CIS) into four groups.[21] Surprisingly, 92% of patients in group 1 were characterized by a subset of 108 genes converted to clinically definite MS (CDMS) within 9 months of the first attack. They suggest downregulation of TOB1, a negative regulator of T cell proliferation as a marker predicting the conversion from CIS to CDMS.

By gene expression profiling with Affymetrix Human Genome U133A2 arrays, Achiron et al. showed that 1578 DEG of peripheral blood mononuclear cells (PBMC) of RRMS patients, differentiating

acute relapse from remission, are enriched in the apoptosis-related pathway, in which proapoptotic genes are downregulated, whereas antiapoptotic genes are upregulated during acute relapse.[22] The same group also compared 62 patients with CDMS and 32 patients with CIS by combining gene expression profiling with the support vector machine (SVM)-based prediction of time to the next acute relapse, setting a two stage predictor composed of First Level Predictors (FLP) and Fine Turning Predictors (FTP).[23] They identified three sets of the best 10-gene FLP that predict the next relapse with a resolution of 500 days and four sets of the best 9-gene FTP that predict the forthcoming relapse with a resolution of 50 days. The predictor genes are enriched in the TGFB2-related signaling pathway. More recently, Achiron et al. compared nine subjects who developed MS during a 9-year follow-up period (the preactive stage of MS; MS-to-be) and 11 control subjects unaffected with MS (MS-free) by gene expression profiling.[24] They found downregulation of nuclear receptor NR4A1 in the preactive stage of MS, suggesting that self-reactive T cells are not eliminated in the MS-to-be population, owing to a defect in the NR4A1-dependent apoptotic mechanism.

By gene expression profiling with a custom microarray of the Peter MacCallum Cancer Institute, Arthur et al. showed that a set of dysregulated genes in peripheral blood cells during the relapse and the remission phases of RRMS are enriched in the categories involved in apoptosis and inflammation, when annotated according to the GOstat program.[25] They also found upregulation of TGFB1 during the relapse. These observations support the working hypothesis that MS relapse involves an imbalance between promoting and preventing apoptosis of autoreactive and regulatory T cells. By gene expression analysis with Affymetrix Human Genome U133 plus 2.0 arrays, Brynedal et al. showed that MS relapses reflect the gene expression change in PBMC, but not in cerebrospinal fluid (CSF) lymphocytes, suggesting the importance of initial events triggering relapses occurring outside the CNS.[26]

By gene expression profiling with a custom DNA microarray (Hitachi Life Science, Saitama, Japan), we identified 43 DEG in peripheral blood $CD3^+$ T cells between the peak of acute relapse and the complete remission of RRMS patients.[27] We isolated highly purified $CD3^+$ T cells, because autoreactive pathogenic and regulatory cells, which potentially play a major role in MS relapse and remission, might be enriched in this fraction. By using 43 DEG as a set of discriminators, hierarchical clustering separated the cluster of relapse from that of remission. The molecular network of 43 DEG extracted by the common upstream search of KeyMolnet showed the most significant relationship with transcriptional regulation by the nuclear factor-kappa B (NF-κB). NF-κB is a central regulator of innate and adaptive immune responses, cell proliferation, and apoptosis.[28] A considerable number of NF-κB target genes activate NF-κB itself, providing a positive regulatory loop that amplifies and perpetuates inflammatory responses, leading to persistent activation of autoreactive T cells in MS. These observations support the logical hypothesis that NF-κB plays a central role in triggering molecular events in T cells responsible for induction of acute relapse of MS, and suggest that aberrant gene regulation by NF-κB on T-cell transcriptome serves as a molecular biomarker for monitoring the clinical disease activity of MS. Supporting this hypothesis, increasing evidence has shown that NF-κB represents a central molecular target for MS therapy.[29]

We also studied the gene expression profile of purified $CD3^+$ T cells isolated from four Hungarian monozygotic MS twin pairs with a custom DNA microarray (Hitachi Life Science, Saitama, Japan).[30] By comparing three concordant pairs and one discordant pair, we identified 20 DEG aberrantly regulated between the MS patient and the genetically identical healthy subject. The molecular network of 20 DEG extracted by the common upstream search of KeyMolnet showed the most significant relationship with transcriptional regulation by the Ets transcription factor family. Ets transcription factor proteins, by interacting with various co-regulatory factors, control the expression of a wide range of target genes essential for cell proliferation, differentiation, transformation and apoptosis. Importantly, Ets-1, the prototype of the Ets family members, acts as a negative regulator of Th17 cell differentiation.[31] It is worthy to note that discordant monozygotic MS twin siblings do not show any genetic or epigenetic differences, as validated by whole genome sequencing analysis and genome-scale DNA methylation profiling.[8]

Biomarkers for predicting IFNβ responders

Although recombinant IFNβ therapy is widely used as the gold standard to reduce disease activity of MS, up to 50% of the patients continue to have relapses, followed by progression of disability. If molecular biomarkers for IFNβ responsiveness are identified, we could use the best treatment options depending on the patients, being invaluable to establish the personalized therapy of MS.

By genome-wide screening of single-nucleotide polymorphisms (SNP) with Affymetrix Human 100K SNP arrays, Byun et al. identified allelic differences between IFNβ responders and non-responders of RRMS patients in several genes, including HAPLN1, GPC5, COL25A1, CAST and NPAS3, although odds ratios of SNP differences of individual genes are fairly low.[32]

By gene expression profiling with Affymetrix Human Genome U133A Plus 2.0 arrays, Comabella et al. showed that IFNβ non-responders of RRMS patients after treatment for 2 years are characterized by the overexpression of type I IFN-induced genes in PBMC, associated with increased endogenous production of type I IFN by monocytes at pretreatment.[33] These observations suggest that a preactivated type I IFN signaling pathway is attributable to IFNβ non-responsiveness in MS. By gene expression profiling with Affymetrix Human Genome Focus arrays, Sellebjerg et al. showed that *in vivo* injection of IFNβ rapidly induces elevation of IFI27, CCL2 and CXCL10 in PBMC of MS patients, even after 6 months of treatment,[34] consistent with previous studies.[35] The induction of IFN-responsive genes is greatly reduced in patients with neutralizing antibodies (NAbs) against IFNβ.[34] In contrast, there exist no global differences in gene expression profiles of PBMC of RRMS patients between NAbs-negative IFNβ non-responders and responders.[36]

By gene expression profiling with Affymetrix Human Genome U133A/B arrays, Goertsches et al. found that IFNβ administration *in vivo* elevates a panel of IFN-responsive genes in PBMC of RRMS patients during a 2-year treatment, but it also downregulates several genes, including CD20, a known target of B-cell depletion therapy in MS.[37] By using the Pathway Architect software (Stratagene, La Jolla, CA, USA), they identified two major gene networks where upregulation of STAT1 and downregulation of ITGA2B act as a central molecule, although they did not further characterize the responder/non-responder-linked gene expression profiles.

By gene expression profiling with a custom array of the National Institutes of Health (NIH)/National Institute of Neurological Disorders and Stroke (NINDS) Microarray Consortium, Fernald et al. showed that a 1-week IFNβ administration *in vivo* induces a set of coregulated genes whose networks are related to immune- and apoptosis-regulatory functions, involving JAK-STAT and NF-κB cascades, whereas the networks of untreated subjects are composed of the genes of cellular housekeeping functions.[38] By combining kinetic RT–PCR analysis of expression of 70 genes in PBMC of RRMS with the integrated Bayesian inference system approach, the same group previously reported that nine sets of gene triplets detected at pretreatment, including a panel of caspases, well predict the response to IFNβ with up to 86% accuracy.[39]

By gene expression profiling with a custom microarary (Hitachi), we previously identified a set of interferon-responsive genes expressed in purified peripheral blood $CD3^+$ T cells of RRMS patients receiving IFNβ treatment.[40] IFNβ immediately induces a burst of expression of chemokine genes with potential relevance to IFNβ-related early adverse effects in MS.[41] The majority of the top 30 most significant DEG in $CD3^+$ T cells between untreated MS patients and healthy subjects are categorized into apoptosis signaling regulators.[42] Furthermore, we found that T cell gene expression profiling classifies a heterogeneous population of Japanese MS patients into four distinct subgroups that differ in the disease activity and therapeutic response to IFNβ.[43] We identified 286 DEG expressed between 72 untreated Japanese MS patients and 22 age- and sex-matched healthy subjects. By importing the list of 286 DEG into the common upstream search of KeyMolnet, the generated network showed the most significant relationship with transcriptional regulation by NF-κB.[30] Although none of the single genes alone serve as a MS-specific biomarker gene, NR4A2 (NURR1), a target of NF-κB acting as a positive regulator of IL-17 and IFNγ production, is highly upregulated in MS T cells.[42,43] It is worthy to note that IFNβ is beneficial in the disease induced by Th1 cells, but detrimental in the disease mediated by Th17 cells in mouse experimental autoimmune encephalomyelitis (EAE), and IFNβ non-responders in RRMS patients show higher serum IL-17F levels, suggesting that IL-17 serves as a biomarker predicting a poor IFNβ response in MS.[44]

Molecular networks of MS brain lesion proteome

Recently, Han et al. investigated a comprehensive proteome of six frozen MS brains.[7] Proteins were prepared from small pieces of brain tissues isolated by laser-captured microdissection (LCM), and they were characterized separately by the standard histological examination, and classified into acute plaques (AP), chronic active plaques (CAP) or chronic plaques (CP) based on the disease activity. The proteins were then separated on one-dimensional SDS-PADE gels, digested in-gel with trypsin, and peptide fragments were processed for mass spectrometric

Table 1 Multiple sclerosis-linked molecules of the KeyMolnet library

KeyMolnet ID	KeyMolnet symbol	Description
KMMC:04422	2,3cnPDE	2',3'-cyclic nucleotide 3'-phosphodiesterase
KMMC:04421	aBcrystallin	Alpha crystallin B chain
KMMC:01024	ADAM17	A disintegrin and metalloproteinase 17
KMMC:04753	AMPAR	AMPA-type glutamate receptor
KMMC:00019	APP	Amyloid beta A4 protein
KMMC:07424	AQP4	Aquaporin 4
KMMC:06672	b-arrestin1	Beta-arrestin 1
KMMC:04017	BAFF	B-cell activating factor
KMMC:00868	Bcl-2	B-cell lymphoma 2
KMMC:00728	Ca	Calcium ion
KMMC:00605	caspase-1	Caspase-1
KMMC:00429	CCL2	Chemokine (C-C motif) ligand 2
KMMC:00425	CCL3	Chemokine (C-C motif) ligand 3
KMMC:00424	CCL5	Chemokine (C-C motif) ligand 5
KMMC:00450	CCR1	Chemokine (C-C motif) receptor 1
KMMC:00454	CCR5	Chemokine (C-C motif) receptor 5
KMMC:03088	CD28	T-cell-specific surface glycoprotein CD28
KMMC:00530	CD80	T-lymphocyte activation antigen CD80
KMMC:03089	CTLA-4	Cytotoxic T-lymphocyte protein 4
KMMC:00418	CXCL10	Chemokine (C-X-C motif) ligand 10
KMMC:00447	CXCR3	Chemokine (C-X-C motif) receptor 3
KMMC:00271	ERa	Estrogen receptor alpha
KMMC:00362	FGF-2	Fibroblast growth factor 2
KMMC:04423	GFAP	Glial fibrillary acidic protein
KMMC:01120	Glu	Glutamic acid
KMMC:00396	glucocorticoid	Glucocorticoid
KMMC:03232	hH1R	Histamine H1 receptor
KMMC:00344	HLA class II	HLA class II histocompatibility antigen
KMMC:09224	HLA-C5	HLA-C5
KMMC:09221	HLA-DQA1*0102	HLA-DQA1*0102
KMMC:06358	HLA-DQA1*0301	HLA-DQA1*0301
KMMC:06359	HLA-DQB1*0302	HLA-DQB1*0302
KMMC:09222	HLA-DQB1*0602	HLA-DQB1*0602
KMMC:06309	HLA-DRB1	HLA-DRB1
KMMC:06315	HLA-DRB1*0301	HLA-DRB1*0301
KMMC:09223	HLA-DRB1*0405	HLA-DRB1*0405
KMMC:09191	HLA-DRB1*11	HLA-DRB1*11
KMMC:07762	HLA-DRB1*15	HLA-DRB1*15
KMMC:06903	HLA-DRB1*1501	HLA-DRB1*1501
KMMC:07763	HLA-DRB1*1503	HLA-DRB1*1503
KMMC:09220	HLA-DRB5*0101	HLA-DRB5*0101
KMMC:04418	HSP105	Heat-shock protein 105 kDa
KMMC:00526	IFNb	Interferon beta
KMMC:00404	IFNg	Interferon gamma
KMMC:00292	IGF1	Insulin-like growth factor 1
KMMC:03611	IgG	Immunoglobulin G
KMMC:00402	IL-10	Interleukin-10
KMMC:03248	IL-12	Interleukin-12
KMMC:04266	IL-12Rb2	Interleukin-12 receptor beta-2 chain
KMMC:03129	IL-17	Interleukin-17
KMMC:03383	IL-18	Interleukin-18
KMMC:00521	IL-1b	Interleukin-1 beta
KMMC:00296	IL-2	Interleukin-2
KMMC:06578	IL-23	Interleukin-23
KMMC:00533	IL-2Rac	Interleukin-2 receptor alpha chain
KMMC:00400	IL-4	Interleukin-4
KMMC:03255	IL-5	Interleukin-5

Table 1 *(Continued)*

KeyMolnet ID	KeyMolnet symbol	Description
KMMC:00108	IL-6	Interleukin-6
KMMC:03257	IL-7Rac	Interleukin-7 receptor alpha chain
KMMC:00523	IL-9	Interleukin-9
KMMC:00555	iNOS	Inducible nitric oxide synthase
KMMC:00982	int-a4/b1	Integrin alpha-4/beta-1
KMMC:00968	int-aM	Integrin alpha-M
KMMC:00970	int-aX	Integrin alpha-X
KMMC:04094	MBP	Myelin basic protein
KMMC:06533	mGluR	Metabotropic glutamate receptor
KMMC:04420	MOG	Myelin-oligodendrocyte glycoprotein
KMMC:04419	MPLP	Myelin proteolipid protein
KMMC:03210	N-VDCC	Voltage dependent N-type calcium channel
KMMC:04712	NCAM	Neural cell adhesion molecule
KMMC:06537	NCE	Na(+)-Ca^{2+} exchanger
KMMC:05576	NeuroF	Neurofilament protein
KMMC:09225	neurofascin	Neurofascin
KMMC:05903	NF-H	Neurofilament triplet H protein
KMMC:05904	NF-L	Neurofilament triplet L protein
KMMC:03785	NMDAR	N-methyl-D-aspartate receptor
KMMC:07764	NMDAR1	N-methyl-D-aspartate receptor subunit NR1
KMMC:07765	NMDAR2C	N-methyl D-aspartate receptor subtype 2C
KMMC:07766	NMDAR3A	N-methyl-D-aspartate receptor subtype NR3A
KMMC:02064	NO	Nitric oxide
KMMC:07767	Olig-1	Oligodendrocyte transcription factor 1
KMMC:01005	OPN	Osteopontin
KMMC:03073	PDGF	Platelet derived growth factor
KMMC:06225	Sema3A	Semaphorin 3A
KMMC:06229	Sema3F	Semaphorin 3F
KMMC:00111	SMAD3	Mothers against decapentaplegic homolog 3
KMMC:03839	tau	Microtubule-associated protein tau
KMMC:00349	TNFa	Tumor necrosis factor alpha
KMMC:00545	VCAM-1	Vascular cell adhesion protein 1
KMMC:03832	VD	Vitamin D
KMMC:03711	VDR	Vitamin D3 receptor

91 multiple sclerosis-linked molecules of the KeyMolnet library are listed in alphabetical order.

analysis. Among 2574 proteins determined with high confidence, the INTERSECT/INTERACT program identified 158, 416 and 236 lesion-specific proteins detected exclusively in AP, CAP and CP, respectively. They found that overproduction of five molecules involved in the coagulation cascade, including tissue factor and protein C inhibitor, plays a central role in molecular events ongoing in CAP. Furthermore, *in vivo* administration of coagulation cascade inhibitors really reduced the clinical severity in EAE, supporting the view that the blockade of the coagulation cascade would be a promising approach for treatment of MS.[43] However, nearly all remaining proteins are uncharacterized in terms of their implications in MS brain lesion development.

We studied molecular networks and pathways of the proteome dataset of Han et al. by using four different bioinformatics tools for molecular network analysis, such as KEGG, PANTHER, KeyMolnet and IPA.[45] KEGG and PANTHER showed the relevance of extracellular matrix (ECM)-mediated focal adhesion and integrin signaling to CAP and CP proteome. KeyMolnet by the N-points to N-points search disclosed a central role of the complex interaction among diverse cytokine signaling pathways in brain lesion development at all disease stages, as well as a role of integrin signaling in CAP and CP. IPA identified the network constructed with a wide range of ECM components, such as COL1A1, COL1A2, COL6A2, COL6A3, FN1, FBLN2, LAMA1, VTN and HSPG2, as one of the networks highly relevant to CAP proteome. Thus, four distinct tools commonly suggested a role of ECM and integrin signaling in development of chronic

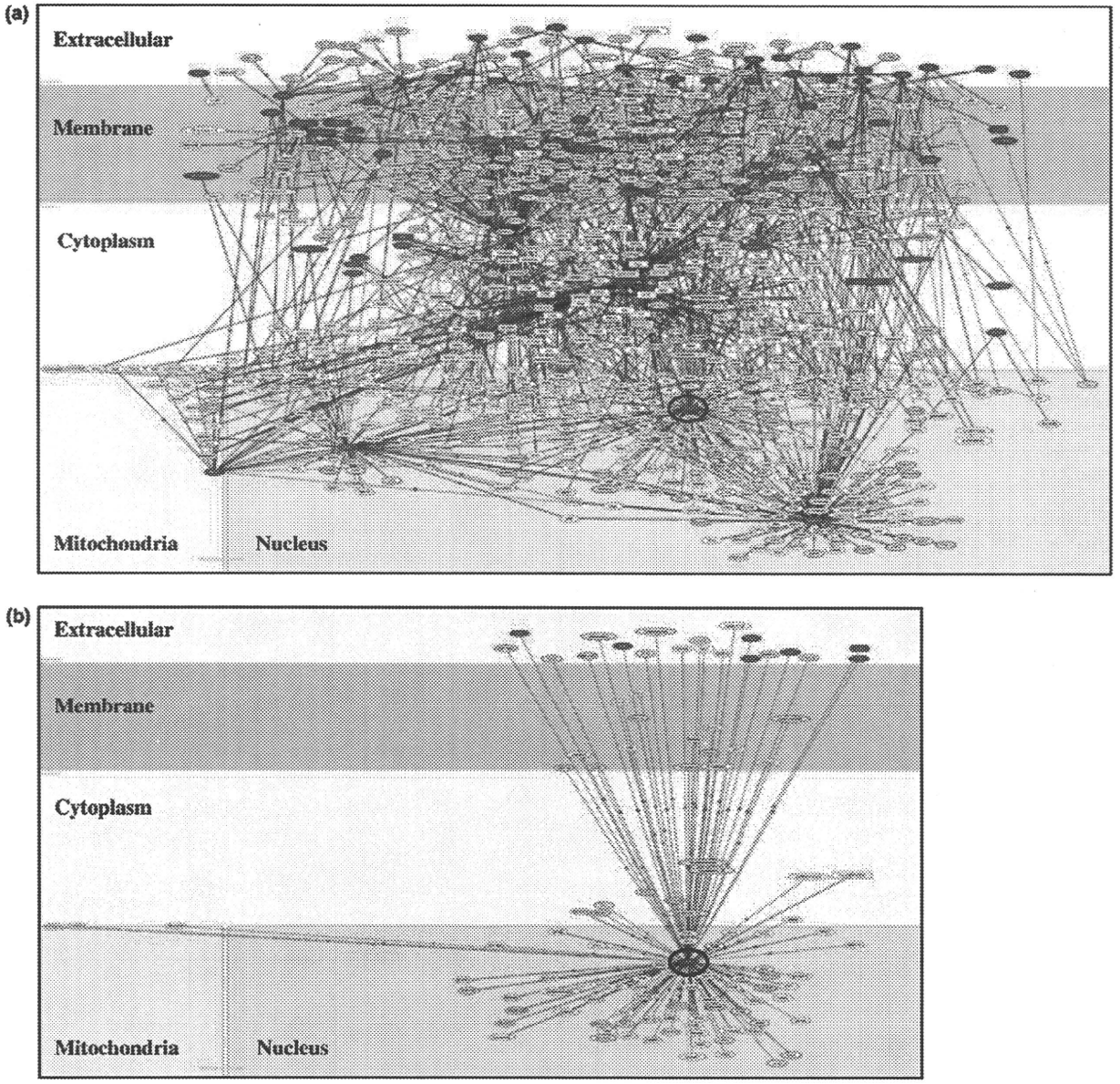

Figure 2 Molecular network of 91 MS-linked molecules. (a) By importing 91 MS-linked molecules into KeyMolnet, the neighboring search within one path from starting points generates the highly complex molecular network composed of 913 molecules and 1005 molecular relations. (b) The extracted network shows the most significant relationship with transcriptional regulation by vitamin D receptor (VDR) that has direct connections with 118 closely related molecules of the extracted network. VDR is indicated by blue circle. Red nodes represent start point molecules, whereas white nodes show additional molecules extracted automatically from core contents to establish molecular connections. The molecular relation is shown by a solid line with an arrow (direct binding or activation), solid line with an arrow and stop (direct inactivation), solid line without an arrow (complex formation), dash line with an arrow (transcriptional activation), and dash line with an arrow and stop (transcriptional repression). Please refer high resolution figures to URL (www.my-pharm.ac.jp/~satoj/sub22.html).

MS lesions, showing that the selective blockade of the interaction between ECM and integrin molecules in brain lesions *in situ* would be a target for therapeutic intervention to terminate ongoing events responsible for the persistence of inflammatory demyelination.

KeyMolnet identifies a candidate of molecular targets for MS therapy

The KeyMolnet library includes 91 MS-linked molecules, collected from selected review articles with the highest reliability (Table 1). By importing the list

Table 2 Molecules constucting the transcriptional regulation by vitamin D receptor network

KeyMolnet ID	KeyMolnet symbol	Description
KMMC:02959	1a,25(OH)2D3	1 alpha, 25-dihydroxyvitamin D3
KMMC:00751	amphiregulin	Amphiregulin
KMMC:03795	ANP	Atrial natriuretic peptide
KMMC:00090	b-catenin	beta-catenin
KMMC:00301	c-Fos	Protooncogene c-fos
KMMC:00183	c-Jun	Protooncogene c-jun
KMMC:00626	c-Myc	Protooncogene c-myc
KMMC:03813	CA-II	Carbonic anhydrase II
KMMC:04105	CalbindinD28K	Vitamin D-dependent calcium-binding protein, avian-type
KMMC:03531	CalbindinD9K	Vitamin D-dependent calcium-binding protein, intestinal
KMMC:00289	caseinK2	Casein kinase 2
KMMC:04195	CaSR	Extracellular calcium-sensing receptor
KMMC:00268	CBP	CREB binding protein
KMMC:00922	CD44	CD44 antigen
KMMC:00136	CDK2	Cyclin dependent kinase 2
KMMC:00135	CDK6	Cyclin dependent kinase 6
KMMC:01008	collagen	Collagen
KMMC:06770	collagenase-I	Type I collagenase
KMMC:04081	CRABP2	Cellular retinoic acid-binding protein II
KMMC:00060	CRT	Calreticulin
KMMC:00401	CXCL8	Chemokine (C-X-C motif) ligand 8 (IL8)
KMMC:00137	cyclinA	Cyclin A
KMMC:00061	cyclinD1	Cyclin D1
KMMC:05926	cyclinD3	Cyclin D3
KMMC:00093	cyclinE	Cyclin E
KMMC:02960	CYP24A1	Cytochrome P450 24A1
KMMC:02958	CYP27B1	Cytochrome P450 27B1
KMMC:04593	CYP3A4	Cytochrome P450 3A4
KMMC:06769	cystatin M	Cystatin M
KMMC:06762	Cytokeratin 13	Keratin, type I cytoskeletal 13
KMMC:06751	Cytokeratin 16	Keratin, type I cytoskeletal 16
KMMC:00053	DHTR	Dihydrotestosterone receptor
KMMC:00928	E-cadherin	E-cadherin
KMMC:00594	ErbB1	Receptor protein-tyrosine kinase erbB-1
KMMC:00068	filamin	Filamin
KMMC:00341	FN1	Fibronectin 1
KMMC:06760	FREAC-1	Forkhead box protein F1
KMMC:06763	G0S2	G0/G1 switch protein 2
KMMC:00617	GM-CSF	Granulocyte macrophage colony stimulating factor
KMMC:06755	Hairless	Hairless protein
KMMC:05978	HOXA10	Homeobox protein Hox-A10
KMMC:06767	HOXB4	Homeobox protein Hox-B4
KMMC:00404	IFNg	Interferon gamma
KMMC:00579	IGF-BP3	Insulin-like growth factor binding protein 3
KMMC:04498	IGF-BP5	Insulin-like growth factor binding protein 5
KMMC:00402	IL-10	Interleukin-10
KMMC:03241	IL-10R	Interleukin-10 receptor
KMMC:03239	IL-10Rac	Interleukin-10 receptor alpha chain
KMMC:03240	IL-10Rbc	Interleukin-10 receptor beta chain
KMMC:03248	IL-12	Interleukin-12
KMMC:03246	IL-12A	Interleukin-12 alpha chain
KMMC:00403	IL-12B	Interleukin-12 beta chain
KMMC:00296	IL-2	Interleukin-2
KMMC:00108	IL-6	Interleukin-6

Table 2 (*Continued*)

KeyMolnet ID	KeyMolnet symbol	Description
KMMC:00973	int-b3	Integrin beta-3
KMMC:03747	IVL	Involucrin
KMMC:00629	JunB	Protooncogene jun-B
KMMC:04334	JunD	Protooncogene jun-D
KMMC:06764	KLK10	Kallikrein-10
KMMC:06765	KLK6	Kallikrein-6
KMMC:04635	Mad1	Max dimerization protein 1
KMMC:06757	Metallothionein	Metallothionein
KMMC:06722	MKP-5	MAP kinase phosphatase 5
KMMC:00595	MMP-2	Matrix metalloproteinase 2
KMMC:03104	MMP-3	Matrix metalloproteinase 3
KMMC:00631	MMP-9	Matrix metalloproteinase 9
KMMC:00556	MnSOD	Manganese superoxide dismutase
KMMC:00927	N-cadherin	N-cadherin
KMMC:00074	NCOA1	Nuclear receptor coactivator 1
KMMC:00075	NCOA2	Nuclear receptor coactivator 2
KMMC:00080	NCOA3	Nuclear receptor coactivator 3
KMMC:00282	NCOR1	Nuclear receptor corepressor 1
KMMC:00270	NCOR2	Nuclear receptor corepressor 2
KMMC:00392	NFAT	Nuclear factor of activated T cells
KMMC:00104	NFkB	Nuclear factor kappa B
KMMC:03120	OPG	Osteoprotegerin
KMMC:01005	OPN	Osteopontin
KMMC:00304	osteocalcin	Osteocalcin
KMMC:00100	p21CIP1	Cyclin dependent kinase inhibitor 1
KMMC:00155	p27KIP1	Cyclin dependent kinase inhibitor 1B
KMMC:00195	p300	E1A binding protein p300
KMMC:03204	PLCb1	Phospholipase C beta 1
KMMC:03295	PLCd1	Phospholipase C delta 1
KMMC:00724	PLCg1	Phospholipase C gamma 1
KMMC:04869	plectin1	Plectin 1
KMMC:06772	PMCA1	Plasma membrane calcium-transporting ATPase 1
KMMC:06766	PP1c	Serine/threonine protein phosphatase PP1 catalytic subunit
KMMC:00786	PP2A	Serine/threonine protein phosphatase 2A
KMMC:03442	PPARd	Peroxisome proliferator activated receptor delta
KMMC:03710	PTH	Parathyroid hormone
KMMC:00346	PTHrP	Parathyroid hormone-related protein
KMMC:03115	RANKL	Receptor activator of NFkB ligand
KMMC:04537	RelB	Transcription factor RelB
KMMC:00091	RIP140	Nuclear factor RIP140
KMMC:00383	RXR	Retinoid X receptor
KMMC:06771	SCCA	Squamous cell carcinoma antigen
KMMC:05340	SKIP	Ski-interacting protein
KMMC:04103	SUG1	26S protease regulatory subunit 8
KMMC:05702	TAFII130	Transcription initiation factor TFIID subunit 4
KMMC:06753	TAFII28	Transcription initiation factor TFIID subunit 11
KMMC:06752	TAFII55	Transcription initiation factor TFIID subunit 7
KMMC:04955	TCF-1	T-cell-specific transcription factor 1
KMMC:03075	TCF-4	T-cell-specific transcription factor 4
KMMC:06754	TFIIA	Transcription initiation factor IIA
KMMC:04089	TFIIB	Transcription initiation factor IIB
KMMC:06768	TGase I	Transglutaminase I
KMMC:04184	TGFb1	Transforming growth factor beta 1
KMMC:05986	TGFb2	Transforming growth factor beta 2
KMMC:04104	TIF1	Transcription intermediary factor 1
KMMC:00349	TNFa	Tumor necrosis factor alpha

Table 2 *(Continued)*

KeyMolnet ID	KeyMolnet symbol	Description
KMMC:00277	TRAP220	Thyroid hormone receptor-associated protein complex component TRAP220
KMMC:06759	TRPV5	TRP vanilloid receptor 5
KMMC:06758	TRPV6	TRP vanilloid receptor 6
KMMC:06756	TRR1	Thioredoxin reductase 1
KMMC:03711	VDR	Vitamin D3 receptor
KMMC:04853	VDUP1	Vitamin D3 up-regulated protein 1
KMMC:06761	ZNF-44	Zinc finger protein 44
KMMC:05147	ZO-1	Tight junction protein ZO-1
KMMC:05811	ZO-2	Tight junction protein ZO-2

118 molecules constucting the transcriptional regulation by VDR network are listed in alphabetical order.

of these molecules into KeyMolnet, the neighboring search within one path from starting points generates the highly complex molecular network composed of 913 molecules and 1005 molecular relations (Fig. 2a). The extracted network shows the most significant relationship with transcriptional regulation by vitamin D receptor (VDR) with *P*-value of the score = 4.415E-242. Thus, VDR, a hub that has direct connections with 118 closely related molecules of the extracted network (Fig. 2b, Table 2), serves as one of the most promising molecular target candidates for MS therapy, because the adequate manipulation of the VDR network capable of producing a great impact on the whole network could efficiently disconnect the pathological network of MS. Indeed, vitamin D plays a protective role in MS by activating VDR, a transcription factor that regulates the expression of as many as 500 genes, although the underlying molecular mechanism remains largely unknown.[46]

Conclusion

MS is a complex disease with remarkable heterogeneity caused by the intricate interplay between various genetic and environmental factors. Recent advances in bioinformatics and systems biology have made major breakthroughs by illustrating the cell-wide map of complex molecular interactions with the aid of the literature-based knowledgebase of molecular pathways. The efficient integration of high-throughput experimental data derived from the disease-affected cells and tissues with underlying molecular networks helps us to characterize the molecular markers and pathways relevant to MS heterogeneity, and promotes us to identify the network-based effective drug targets for personalized therapy of MS.

Acknowledgements

This work was supported by grants from the Research on Intractable Diseases, the Ministry of Health, Labour and Welfare of Japan (H22-Nanchi-Ippan-136), and the High-Tech Research Center Project, the Ministry of Education, Culture, Sports, Science and Technology (MEXT), Japan (S0801043). The author thanks Dr Takashi Yamamura, Department of Immunology, National Institute of Neurosciences, NCNP for his continuous help with our studies.

References

1. Sospedra M, Martin R. Immunology of multiple sclerosis. *Annu Rev Immunol.* 2005; **23**: 683–747.
2. Steinman L. A brief history of T_H17, the first major revision in the T_H1/T_H2 hypothesis of T cell-mediated tissue damage. *Nat Med.* 2007; **13**: 139–45.
3. Lucchinetti C, Brück W, Parisi J, Scheithauer B, Rodriguez M, Lassmann H. Heterogeneity of multiple sclerosis lesions: implications for the pathogenesis of demyelination. *Ann Neurol.* 2000; **47**: 707–17.
4. Rudick RA, Lee JC, Simon J, Ransohoff RM, Fisher E. Defining interferon β response status in multiple sclerosis patients. *Ann Neurol.* 2004; **56**: 548–55.
5. International Multiple Sclerosis Genetics Consortium, Hafler DA, Compston A, Sawcer S, Lander ES, Daly MJ, et al. Risk alleles for multiple sclerosis identified by a genomewide study. *N Engl J Med.* 2007; **357**: 851–62.
6. Lock C, Hermans G, Pedotti R, Brendolan A, Schadt E, Garren H, et al. Gene-microarray analysis of multiple sclerosis lesions yields new targets validated in autoimmune encephalomyelitis. *Nature Med.* 2002; **8**: 500–8.
7. Han MH, Hwang SI, Roy DB, Lundgren DH, Price JV, Ousman SS, et al. Proteomic analysis of active multiple sclerosis lesions reveals therapeutic targets. *Nature.* 2008; **451**: 1076–81.

8. Baranzini SE, Mudge J, van Velkinburgh JC, Khankhanian P, Khrebtukova I, Miller NA, et al. Genome, epigenome and RNA sequences of monozygotic twins discordant for multiple sclerosis. *Nature*. 2010; **464**: 1351–6.
9. Viswanathan GA, Seto J, Patil S, Nudelman G, Sealfon SC. Getting started in biological pathway construction and analysis. *PLoS Comput Biol*. 2008; **4**: e16.
10. Kitano H. A robustness-based approach to systems-oriented drug design. *Nat Rev Drug Discov*. 2007; **6**: 202–10.
11. Albert R, Jeong H, Barabasi AL. Error and attack tolerance of complex networks. *Nature*. 2000; **406**: 378–82.
12. Satoh J, Tabunoki H, Arima K. Molecular network analysis suggests aberrant CREB-mediated gene regulation in the Alzheimer disease hippocampus. *Dis Markers*. 2009; **27**: 239–52.
13. MAQC Consortium, Shi L, Reid LH, Jones WD, Shippy R, Warrington JA, et al. The MicroArray Quality Control (MAQC) project shows inter- and intraplatform reproducibility of gene expression measurements. *Nat Biotechnol*. 2006; **24**: 1151–61.
14. Huang DW, Sherman BT, Lempicki RA. Systematic and integrative analysis of large gene lists using DAVID bioinformatics resources. *Nat Protoc*. 2009; **4**: 44–57.
15. Subramanian A, Tamayo P, Mootha VK, Mukherjee S, Ebert BL, Gillette MA, et al. Gene set enrichment analysis: a knowledge-based approach for interpreting genome-wide expression profiles. *Proc Natl Acad Sci USA*. 2005; **102**: 15545–50.
16. Kanehisa M, Goto S, Furumichi M, Tanabe M, Hirakawa M. KEGG for representation and analysis of molecular networks involving diseases and drugs. *Nucleic Acids Res*. 2010; **38**: D355–60.
17. Mi H, Dong Q, Muruganujan A, Gaudet P, Lewis S, Thomas PD. PANTHER version 7: improved phylogenetic trees, orthologs and collaboration with the Gene Ontology Consortium. *Nucleic Acids Res*. 2010; **38**: D204–10.
18. Jensen LJ, Kuhn M, Stark M, Chaffron S, Creevey C, Muller J, et al. STRING 8 – a global view on proteins and their functional interactions in 630 organisms. *Nucleic Acids Res*. 2009; **37**: D412–6.
19. Pospisil P, Iyer LK, Adelstein SJ, Kassis AI. A combined approach to data mining of textual and structured data to identify cancer-related targets. *BMC Bioinformatics*. 2006; **7**: 354.
20. Sato H, Ishida S, Toda K, Matsuda R, Hayashi Y, Shigetaka M, et al. New approaches to mechanism analysis for drug discovery using DNA microarray data combined with KeyMolnet. *Curr Drug Discov Technol*. 2005; **2**: 89–98.
21. Corvol JC, Pelletier D, Henry RG, Caillier SJ, Wang J, Pappas D, et al. Abrogation of T cell quiescence characterizes patients at high risk for multiple sclerosis after the initial neurological event. *Proc Natl Acad Sci USA*. 2008; **105**: 11839–44.
22. Achiron A, Feldman A, Mandel M, Gurevich M. Impaired expression of peripheral blood apoptotic-related gene transcripts in acute multiple sclerosis relapse. *Ann N Y Acad Sci*. 2007; **1107**: 155–67.
23. Gurevich M, Tuller T, Rubinstein U, Or-Bach R, Achiron A. Prediction of acute multiple sclerosis relapses by transcription levels of peripheral blood cells. *BMC Med Genomics*. 2009; **2**: 46.
24. Achiron A, Grotto I, Balicer R, Magalashvili D, Feldman A, Gurevich M. Microarray analysis identifies altered regulation of nuclear receptor family members in the pre-disease state of multiple sclerosis. *Neurobiol Dis*. 2010; **38**: 201–9.
25. Arthur AT, Armati PJ, Bye C; Southern MS Genetics Consortium, Heard RN, Stewart GJ, et al. Genes implicated in multiple sclerosis pathogenesis from consilience of genotyping and expression profiles in relapse and remission. *BMC Med Genet*. 2008; **9**: 17.
26. Brynedal B, Khademi M, Wallström E, Hillert J, Olsson T, Duvefelt K. Gene expression profiling in multiple sclerosis: a disease of the central nervous system, but with relapses triggered in the periphery? *Neurobiol Dis*. 2010; **37**: 613–21.
27. Satoh J, Misawa T, Tabunoki H, Yamamura T. Molecular network analysis of T-cell transcriptome suggests aberrant regulation of gene expression by NF-κB as a biomarker for relapse of multiple sclerosis. *Dis Markers*. 2008; **25**: 27–35.
28. Barnes PJ, Karin M. Nuclear factor-κB. A pivotal transcription factor in chronic inflammatory diseases. *N Engl J Med*. 1997; **336**: 1066–71.
29. Yan J, Greer JM. NF-κB, a potential therapeutic target for the treatment of multiple sclerosis. *CNS Neurol Disord Drug Targets*. 2008; **7**: 536–57.
30. Satoh J, Illes Z, Peterfalvi A, Tabunoki H, Rozsa C, Yamamura T. Aberrant transcriptional regulatory network in T cells of multiple sclerosis. *Neurosci Lett*. 2007; **422**: 30–3.
31. Du C, Liu C, Kang J, Zhao G, Ye Z, Huang S, et al. MicroRNA miR-326 regulates T_H-17 differentiation and is associated with the pathogenesis of multiple sclerosis. *Nat Immunol*. 2009; **10**: 1252–9.
32. Byun E, Caillier SJ, Montalban X, Villoslada P, Fernández O, Brassat D, et al. Genome-wide pharmacogenomic analysis of the response to interferon beta therapy in multiple sclerosis. *Arch Neurol*. 2008; **65**: 337–44.
33. Comabella M, Lünemann JD, Río J, Sánchez A, López C, Julià E, et al. A type I interferon signature in monocytes is associated with poor response to interferon-β in multiple sclerosis. *Brain*. 2009; **132**: 3353–65.
34. Sellebjerg F, Krakauer M, Hesse D, Ryder LP, Alsing I, Jensen PE, et al. Identification of new sensitive biomarkers for the *in vivo* response to interferon-β treatment in multiple sclerosis using DNA-array evaluation. *Eur J Neurol*. 2009; **16**: 1291–8.

35. Weinstock-Guttman B, Badgett D, Patrick K, Hartrich L, Santos R, Hall D, et al. Genomic effects of IFN-β in multiple sclerosis patients. *J Immunol.* 2003; **171**: 2694–702.
36. Hesse D, Krakauer M, Lund H, Søndergaard HB, Langkilde A, Ryder LP, et al. Breakthrough disease during interferon-β therapy in MS: no signs of impaired biologic response. *Neurology.* 2010; **74**: 1455–62.
37. Goertsches RH, Hecker M, Koczan D, Serrano-Fernandez P, Moeller S, Thiesen HJ, et al. Long-term genome-wide blood RNA expression profiles yield novel molecular response candidates for IFN-β-1b treatment in relapsing remitting MS. *Pharmacogenomics.* 2010; **11**: 147–61.
38. Fernald GH, Knott S, Pachner A, Caillier SJ, Narayan K, Oksenberg JR, et al. Genome-wide network analysis reveals the global properties of IFN-β immediate transcriptional effects in humans. *J Immunol.* 2007; **178**: 5076–85.
39. Baranzini SE, Mousavi P, Rio J, Caillier SJ, Stillman A, Villoslada P, et al. Transcription-based prediction of response to IFNβ using supervised computational methods. *PLoS Biol.* 2005; **3**: e2.
40. Koike F, Satoh J, Miyake S, Yamamoto T, Kawai M, Kikuchi S, et al. Microarray analysis identifies interferon beta-regulated genes in multiple sclerosis. *J Neuroimmunol.* 2003; **139**: 109–18.
41. Satoh J, Nanri Y, Tabunoki H, Yamamura T. Microarray analysis identifies a set of CXCR3 and CCR2 ligand chemokines as early IFNbeta-responsive genes in peripheral blood lymphocytes in vitro: an implication for IFNbeta-related adverse effects in multiple sclerosis. *BMC Neurol.* 2006; **6**: 18.
42. Satoh J, Nakanishi M, Koike F, Miyake S, Yamamoto T, Kawai M, et al. Microarray analysis identifies an aberrant expression of apoptosis and DNA damage-regulatory genes in multiple sclerosis. *Neurobiol Dis.* 2005; **18**: 537–50.
43. Satoh J, Nakanishi M, Koike F, Onoue H, Aranami T, Yamamoto T, et al. T cell gene expression profiling identifies distinct subgroups of Japanese multiple sclerosis patients. *J Neuroimmunol.* 2006; **174**: 108–18.
44. Axtell RC, de Jong BA, Boniface K, van der Voort LF, Bhat R, De Sarno P, et al. T helper type 1 and 17 cells determine efficacy of interferon-β in multiple sclerosis and experimental encephalomyelitis. *Nat Med.* 2010; **16**: 406–12.
45. Satoh JI, Tabunoki H, Yamamura T. Molecular network of the comprehensive multiple sclerosis brain-lesion proteome. *Mult Scler.* 2009; **15**: 531–41.
46. Ascherio A, Munger KL, Simon KC. Vitamin D and multiple sclerosis. *Lancet Neurol.* 2010; **9**: 599–612.